ASIAN JOURNAL OF PHARMACEUTICAL AND CLINICAL RESEARCH

INNOVARE ACADEMIC SCIENCES
Knowledge to Innovation

Vol 19, Issue 1, 2026

Online - 2455-3891
Print - 0974-2441

Research Article

DESIGN-DRIVEN DISCOVERY OF 3,5-DISUBSTITUTED HYDANTOIN-BASED ANTICONVULSANTS SUPPORTED BY *IN VIVO* AND *IN SILICO* STUDIES

DANDAMUDI ALEKHYA[1,2]*, KONDA RAVI KUMAR[3], NAGARAJU PAPPULA[4]

[1]Department of Pharmacy, Acharya Nagarjuna University, Guntur, Andhra Pradesh, India. [2]Department of Pharmaceutical Chemistry, Krishna University College of Pharmaceutical Sciences and Research, Machilipatnam, Andhra Pradesh, India. [3]Department of Pharmaceutical Chemistry, Hetero Institute of Pharmaceutical Sciences, Gangaram, Telangana, India. [4]Professor and HOD, Department of Pharmaceutical Analysis, Hindu College of Pharmacy, Guntur, Andhra Pradesh, India.
***Corresponding author: Dandamudi Alekhya; Email: dandamudialekhya@gmail.com**

Received: 07 August 2025, Revised and Accepted: 23 October 2025

ABSTRACT

Objectives: The present study aimed to synthesize a series of imidazolidine-2,4-dione (hydantoin) derivatives 5a–5g containing an indole moiety and to evaluate their anticonvulsant potential both *in vivo* and *in silico*. The study further sought to explore structure–activity relationships and predict the binding interactions of these compounds with the voltage-gated sodium channel protein (PDB ID: 3RVY).

Methods: The target compounds 5a–5g were synthesized using standard synthetic methodologies and characterized through physical and spectral analyses. Wistar albino rats were used to assess the *in vivo* anticonvulsant activity employing maximal electroshock (MES) and pentylenetetrazole (PTZ) seizure models, with phenytoin serving as the reference drug. In addition, molecular docking studies were performed using AutoDockVina to evaluate the binding affinities of the synthesized compounds at the sodium channel active site.

Results: All synthesized compounds were obtained in good yields and confirmed through spectral analyses. *In vivo* testing showed that compounds 5c and 5d exhibited the highest percent protection in the PTZ (5c: 83.33%, 5d: 66.66%) and MES (5c: 83.33%, 5d: 83.33%) models. Molecular docking results revealed strong predicted binding affinities for compound 5b (–9.5 kcal/mol) and compounds 5c and 5d (–9.1 kcal/mol each) at the sodium channel target, which were comparable to or better than the reference ligand phenytoin.

Conclusion: Both *in vivo* anticonvulsant activity and *in silico* molecular docking studies indicated that electron-withdrawing nitro-substituted compounds, particularly 5c and 5d, possess significant anticonvulsant potential and strong binding affinity at the sodium channel active site. These findings highlight the promise of nitro-substituted hydantoin derivatives as lead compounds for further pharmacological optimization and development as anticonvulsant agents.

Keywords: N-methylurea, Glyoxal, 1-methyl-imidazolidine-2,4-dione, Indole-3-aldehyde, Hydantoin bearing indole, Anticonvulsant activity, Docking studies.

 DOI: http://dx.doi.org/10.22159/ajpcr.2026v19i1.56413. Journal homepage: https://innovareacademics.in/journals/index.php/ajpcr

INTRODUCTION

Heterocyclic compounds play a vital role in pharmaceutical chemistry due to their diverse biological activities and structural versatility. These compounds, which feature rings containing at least one atom other than carbon (such as nitrogen, oxygen, or sulfur), are a cornerstone of drug discovery and development. Heterocyclic compounds provide a wide range of chemical structures, enabling the design of molecules with specific biological activities. Many natural products, such as alkaloids, flavonoids, and antibiotics, contain heterocyclic moieties, making them a natural template for drug development [1]. Heterocycles enhance the pharmacokinetic properties (absorption, distribution, metabolism, and excretion) of drugs. They serve as bioisosteres, replacing non-cyclic or other cyclic groups to optimize the biological activity of lead compounds. Pyrrole, pyridine, pyrimidine, imidazole, pyrazole, etc., are nitrogen-containing heterocycles frequently found in drugs due to their role in hydrogen bonding and receptor binding [2]. Furan, pyran, oxazole, etc., are oxygen-containing heterocycles that are often linked with antifungal, antibacterial, and anticancer properties. Thiophene, thiazole, etc., are sulfur-containing heterocycles that exhibit a range of activities, including anti-inflammatory and antimicrobial effects [3]. Advances in synthetic organic chemistry have made it easier to design and synthesize heterocyclic compounds with desired properties, enhancing their potential as drug candidates. Heterocycles are crucial for understanding drug-receptor interactions, enzyme inhibition, and other biological mechanisms, aiding rational drug design. The importance of heterocyclics in pharmaceutical chemistry lies in their unmatched ability to combine structural complexity, biological activity, and therapeutic versatility. They are indispensable tools in the arsenal of medicinal chemists working to address diverse healthcare challenges [4].

Hydantoins are a class of heterocyclic organic compounds containing a five-membered ring structure with two nitrogen atoms and a keto group, typically represented by the molecular formula $C_3H_4N_2O_2$. The hydantoin core structure is derived from imidazolidine-2,4-dione. These compounds are of significant interest in medicinal chemistry, agriculture, and material science due to their versatile biological and chemical properties. The hydantoin ring is a cyclic urea and amino acid derivative, consisting of an imidazolidine ring with keto groups at positions 2 and 4. Modifications at the 3 and 5 positions allow for the synthesis of various derivatives with specific chemical and biological properties [5]. Hydantoins are relatively stable compounds due to resonance stabilization of their cyclic structure. Hydantoins have been extensively studied for their pharmacological activities. The most well-known hydantoin derivative is phenytoin, widely used as an anticonvulsant for the treatment of epilepsy by stabilizing neuronal membranes and reducing excitability. Certain hydantoins exhibit antibacterial and antifungal properties, making them useful in combating infections. Some hydantoin derivatives act as anti-inflammatory drugs, offering potential in treating inflammatory diseases [6]. Modified hydantoins have shown promise in targeting cancer cells due to their

cytotoxic activity. Hydantoins serve as a scaffold for designing a wide range of bioactive molecules. The versatility of substitution on the hydantoin ring makes it a valuable template in medicinal chemistry. Hydantoin derivatives often exhibit favorable pharmacokinetic profiles, including good oral bioavailability and metabolic stability. In addition to pharmaceutical applications, hydantoins are used in agriculture as plant growth regulators and herbicides [7].

Hydantoins are synthesized through a variety of methods, including the Bucherer–Bergs reaction, which involves the condensation of aldehydes or ketones with ammonium carbonate and cyanides; cyclization reactions of amino acids with urea derivatives; the Urech or Read synthesis; and the Biltz reaction. Hydantoins are a chemically and biologically significant class of compounds with a wide array of applications in medicine, agriculture, and industry. Their ability to act as pharmacophores and their structural adaptability make them a critical focus in drug discovery and development [8].

Hydantoin scaffolds bearing an indole moiety were the main goal of this investigation. A number of hydantoin derivatives were produced by the Mannich reaction, which involved combining 1-methyl hydantoin with formaldehyde, substituted aromatic amines, and a catalytic quantity of concentrated HCl. The newly synthesized hydantoin derivatives were categorized using spectroscopic and physical properties. To evaluate the effects or dangers of these substances, tested for anticonvulsant activity using pentylenetetrazole (PTZ) and maximal electroshock (MES) induced seizures in *Wistar albino* rats. Using *in silico* molecular docking experiments, the binding interaction at active site regions of the voltage-gated sodium channel (PDB ID: 3RVY) was examined in order to anticipate anticonvulsant effects.

METHODS

Every chemical needed to synthesize the new hydantoins, including solvents and reagents, was purchased from Merck-grade commercial vendors and utilized unpurified. Using E. Merck grade silica gel 60GF-254 pre-coated thin-layer chromatography (TLC) plates, TLC was used to track the progress and completion of the reaction. Spots were seen in an iodine chamber and under ultraviolet light. By employing the KBr pressed pellet technique to compress the compound with anhydrous KBr under vacuum, the Fourier transform infrared spectroscopy (FT-IR) spectra of the compounds were captured on a Bruker FT-IR analyzer spectrophotometer. Chemical shifts in δ, ppm of ^{1}H-NMR spectra were recorded on a Bruker AMX400 MHz spectrometer using deuterated dimethyl sulfoxide (DMSO) solvent and tetramethylsilane as internal standard. Mass spectra of the compounds were recorded on an Agilent LC-MSD 1200 mass spectrometer. Utilizing electrical melting point equipment, melting points have been determined and left uncorrected. *In vivo* anticonvulsant activity was performed on *Wistar albino* rats using PTZ and maximal electroshock (MES) methods. Using the software programs AutoDockVina, ChemDraw, and BIOVIA Discovery Studio, molecular docking investigations were performed at several target protein active sites.

Instruments/equipment/apparatus/software used

Merck-grade reagents, E. Merck grade silica gel 60GF- 254 pre-coated TLC plates, Bruker FT-IR spectrophotometer, Bruker AMX400 MHz spectrometer Agilent LC-MSD 1200 mass spectrometer; Softwares AutoDock Vina, ChemDraw, and BIOVIA Discovery Studio for molecular docking investigations.

Experimental work

Synthesis of 1-methyl-imidazolidine-2,4-dione(3)

As the scheme illustrates, using phosphoric acid as a catalyst, dissolve 0.01 mol of glyoxal (1) and 0.01 mol of N-methyl urea (2) in 15–20 mL of water, then transfer the mixture into a 100 mL round-bottomed flask. To obtain 1-methyl-imidazolidine-2,4-dione, the reaction was conducted for 10–20 min at room temperature in aqueous solutions, providing gentle and environmentally friendly conditions. TLC was used to track the reaction development. Once the reaction was finished, the reaction mixture was added to 25 mL of water. Ethanol was used to recrystallize the product by following the standard workup [9,10].

78.68% yield, pale yellow crystalline powder, melting point 156–158°C, R_f value 0.58 from using chloroform and methanol (7:3). IR [KBr ν cm^{-1}]: 3317 (-NH-), 1726, 1718 (C=O), 2962 (C-H), 1301 (C-N). ^{1}H-NMR [400 MHz, δ, ppm, DMSO-d_6]: 11.85 (s, 1H, hydantoin-NH), 4.11 (s, 2H, CH_2), 3.51 (s, 3H, CH_3). ^{13}C-NMR [100 MHz, δ, ppm, DMSO-d_6]: 174, 170, 45, 33. ESI-MS: (M^+) m/z 114.

Synthesis of 5-[(indol-3-yl)methylene]-1-methyl-imidazolidine-2,4-dione (4)

1-methyl-imidazolidine-2,4-dione (0.01 mol, compound 3) was added to an 8 mL solution of indole-3-carboxaldehyde (0.01 mol) in toluene. After adding 0.4 mL of piperidine catalytically, the reaction mixture was refluxed for 5–6 h at 110–120°C in an oil bath. TLC kept monitoring the reaction's development. After finishing, the mixture was allowed to cool to ambient temperature before 1 M HCl and cold water were added. Filtration was used to collect the precipitate, which was then cleaned with cold water and dry toluene in succession before being dried. Through recrystallization from ethanol, the crude product was further processed [11,12].

Compound (4) was obtained as dark yellow powder analyzed for the yield 72.24%, mp192–194°C, R_f value – 0.53 from TLC of benzene and ethyl acetate (8:2). IR spectrum showed the characteristic intense bands at 3308.20 cm^{-1} (-NH-), 3249.88 cm^{-1} (-NH-), 1664.87 cm^{-1} (C=O), 1738.18 cm^{-1} (C=O), 1332.52 cm^{-1} (C-N), 3025.18 cm^{-1} (=CH), 2948.51 (C-H) and 1678.44 cm^{-1} (C=C). The ^{1}H-NMR spectrum showed the characteristic signals at 400 MHz in DMSO-d_6 with δ 12.40 (1H, s, hydantoin-NH-), δ 12.11 (1H, s, indole-NH-), δ 8.16 (1H, s, =CH- methylene), δ 7.21–7.95 (5H, d and t, indole-H), 3.42 (3H, s, CH_3). The ^{13}C-NMR spectrum showed the characteristic signals at 100 MHz in DMSO-d_6 with δ 169, δ 167, δ 138, δ 130, δ 127, δ 125, δ 123, δ 120, δ 117, δ 115, δ 111, δ 108, and δ 38. The mass spectrum of the compound (4) was further confirmed with ESI-MS: m/z (M^+) 241.

Synthesis of 3-substituted-5-[(indol-3-yl)methylene]-1-methyl-imidazolidine-2,4-dione derivatives(5a–5g)

The formaldehyde (0.01 mol) was added to a 5-[(indol-3-yl)methylene]-1-methyl-imidazolidine-2,4-dione (4) solution in DMF. Stir for about half an hour at room temperature. After pouring the aryl amine (0.01 mol) solution in DMF over the reaction mixture, three to five drops of

Category	Instrument/equipment/apparatus	Model	Manufacturer
Reagents	Analytical grade chemicals	Merck grade	Merck KGaA, Germany
TLC	Silica gel 60 GF254 pre-coated plates	E. Merck grade	E. Merck, Germany
FT-IR spectrophotometer	FT-IR analyzer	Bruker Alpha-II	BrukerOptik GmbH, Germany
NMR spectrometer	AMX400 MHz	Bruker AMX400	BrukerBioSpin GmbH, Germany
Mass spectrometer	LC-MSD 1200	Agilent LC-MSD 1200	Agilent Technologies, USA
Melting point apparatus	Contemp melting point apparatus	MEPOAP121	Contemporary Export Industries
Docking software	Computer software	AutoDockVina	Scripps Research Institute
Chemical drawing	ChemDraw	ChemDraw Ultra 12.0	PerkinElmer Informatics, USA
Molecular modeling	BIOVIA Discovery Studio	BIOVIA Studio Visualizer 2021	DassaultSystèmes BIOVIA, USA

TLC: Thin-layer chromatography, FT-IR: Fourier transform infrared spectroscopy

concentrated HCl were added catalytically. After refluxing for 10–14 h at 120°C, the resultant reaction mixture was chilled for around 24 h at 2–8°C. After adding the reaction mixture to crushed ice and filtering the solid, it was cleaned with cold water and dry toluene. After drying, the product was separated from the ethanol and recrystallized. The reaction's progress was tracked by TLC using a 9:1 n-hexane: ethyl acetate eluent [13,14].

5-[(1H-indol-3-yl)methylene]-3-[(4-bromophenyl)aminomethyl]-1-methylimidazolidine-2,4-dione(5a)

Compound (5a) was obtained as pale yellow powder analyzed for the yield 68.42%, mp 184–186°C, R_f value is 0.53 from TLC of n-hexane and ethylacetate (9:1). IR spectrum (KBr ν cm^{-1}) showed the characteristic intense bands at 3386 (-NH-), 3228 (-NH-), 1745 (C=O), 1768 (C=O), 1305 (C-N), 2975 (C-H), 3045 (=C-H), 536 (C-Br). ^{1}H-NMR [400 MHz, δ, ppm, DMSO-d_6]: 12.14 (1H, s, indole-NH-), 8.16 (1H, s, =CH- methylene), 7.16–7.87 (9H, d and t, phenyl-H and indole-H), 5.11–5.20 (1H, t, -CH_2-NH-), 4.30–4.32 (2H, d, -CH_2-NH-), 3.47 (3H, s, CH_3). ^{13}C-NMR [100 MHz, δ, ppm, DMSO-d_6]: 176, 164, 147, 144, 139, 134, 130, 127, 126, 124, 120, 118, 116, 113, 111, 108, 64, 42. ESI-MS: m/z (M^+) 424.

5-[(1H-indol-3-yl)methylene]-3-[(4-chlorophenyl)aminomethyl]-1-methylimidazolidine-2,4-dione(5b)

Compound (5b) was obtained as light yellow powder analyzed for the yield 70.25%, mp 190–192°C, R_f value is 0.57 from TLC of n-hexane and ethylacetate (9:1). IR spectrum (KBr ν cm^{-1}) showed the characteristic intense bands at 3339 (-NH-), 3237 (-NH-), 1739 (C=O), 1757 (C=O), 1319 (C-N), 2988 (C-H), 3033 (=C-H), 875 (C-Cl). ^{1}H-NMR [400 MHz, δ, ppm, DMSO-d_6]: 12.20 (1H, s, indole-NH-), 8.39 (1H, s, =CH- methylene), 6.90–8.14 (9H, d and t, phenyl-H and indole-H), 4.70-4.73 (2H, d, -CH_2-NH-), 4.19–4.30 (1H, t, -CH_2-NH-), 3.58 (3H, s, CH_3). ^{13}C-NMR [100 MHz, δ, ppm, DMSO-d_6]: 175, 167, 148, 145, 137, 130, 127, 125, 124, 122.0, 121, 119, 115, 113, 111, 108, 66, 39. ESI-MS: m/z (M^+) 380.

5-[(1H-indol-3-yl)methylene]-3-[(4-nitrophenyl)aminomethyl]-1-methylimidazolidine-2,4-dione (5c)

Compound (5c) was obtained as dark yellow powder analyzed for the yield 69.10%, mp 204–206°C, R_f value is 0.62 from TLC of n-hexane and ethylacetate (9:1). IR spectrum (KBr ν cm^{-1}) showed the characteristic intense bands at 3382 (-NH-), 3255 (-NH-), 1756 (C=O), 1734 (C=O), 1329 (C-N), 2975 (C-H), 3052 (=C-H), 1545 and 1338 (-NO_2). ^{1}H-NMR [400 MHz, δ, ppm, DMSO-d_6]: 12.49 (1H, s, indole-NH-), 8.19 (1H, s, =CH- methylene), 7.21-7.99 (9H, d and t, phenyl-H and indole-H), 5.12–5.23 (1H, t, -CH_2-NH-), 4.30–4.33 (2H, d, -CH_2-NH-), 3.62 (3H, s, CH_3). ^{13}C-NMR [100 MHz, δ, ppm, DMSO-d_6]: 176, 165, 156, 145, 138, 135, 130, 128, 126, 124, 121, 118, 116, 115, 113, 111, 68, 40. ESI-MS: m/z (M^+) 391.

5-[(1H-indol-3-yl)methylene]-3-[(2,4-dinitrophenyl)aminomethyl]-1-methylimidazolidine-2,4-dione (5d)

Compound (5d) was obtained as light brown powder analyzed for the yield 73.41%, mp 194–196°C, R_f value is 0.54 from TLC of n-hexane and ethylacetate (9:1). IR spectrum (KBr ν cm^{-1}) showed the characteristic intense bands at 3356 (-NH-), 3242 (-NH-), 1772 (C=O), 1762 (C=O), 1337 (C-N), 2955 (C-H), 3102 (=C-H), 618.45 (C-S), 1668.65 (C=C), 1555 and 1356 (-NO_2). ^{1}H-NMR [400 MHz, δ, ppm, DMSO-d_6]: 11.87 (1H, s, indole-NH-), 8.39 (1H, s, =CH- methylene), 6.68–8.14 (8H, s, d and t, phenyl-H and indole-H), 4.71-4.74 (2H, d, -CH_2-NH-), 4.11–4.20 (1H, t, -CH_2-NH-), 3.26 (3H, s, CH_3). ^{13}C-NMR [100 MHz, δ, ppm, DMSO-d_6]: 176, 167, 152, 145, 138, 136, 133, 130, 129, 126, 124, 122, 120, 118, 116, 114, 110, 109, 69, 46. ESI-MS: m/z (M^+) 436.

5-[(1H-indol-3-yl)methylene]-3-[(4-tolyl)aminomethyl]-1-methylimidazolidine-2,4-dione (5e)

Compound (5e) was obtained as pale yellow powder analyzed for the yield 70.67%, mp 188–190°C, R_f value is 0.51 from TLC of n-hexane and ethylacetate (9:1). IR spectrum (KBr ν cm^{-1}) showed the characteristic intense bands at 3366 (-NH-), 3260 (-NH-), 1747 (C=O), 1735 (C=O), 1344 (C-N), 2960 (C-H), 3074 (=C-H). ^{1}H-NMR [400 MHz, δ, ppm, DMSO-d_6]: 11.98 (1H, s, indole-NH-), 8.23 (1H, s, =CH- methylene), 6.78–7.89 (9H, d and t, phenyl-H and indole-H), 4.42–4.53 (1H, t, -CH_2-NH-), 4.19–4.25 (2H, d, -CH_2-NH-), 2.43 (3H, s, phenyl-CH_3), 3.38 (3H, s, CH_3). ^{13}C-NMR [100 MHz, δ, ppm, DMSO-d_6]: 176, 168, 147, 143, 138, 132, 130, 128, 126, 123, 121, 118, 116, 114, 112, 110, 63, 32, 28. ESI-MS: m/z (M^+) 360.

5-[(1H-indol-3-yl)methylene]-3-[(4-methoxyphenyl)aminomethyl]-1-methylimidazolidine-2,4-dione (5f)

Compound (5f) was obtained as yellowish brown powder analyzed for the yield 68.36%, mp 200–202°C, R_f value is 0.56 from TLC of n-hexane and ethylacetate (9:1). IR spectrum (KBr ν cm^{-1}) showed the characteristic intense bands at 3346 (-NH-), 3245 (-NH-), 1758 (C=O), 1741 (C=O), 1350 (C-N), 2966 (C-H), 3059 (=C-H), 1130 (C-O-C). ^{1}H-NMR [400 MHz, δ, ppm, DMSO-d_6]: 12.13 (1H, s, indole-NH-), 8.20 (1H, s, =CH- methylene), 6.90–7.92 (9H, d and t, phenyl-H and indole-H), 4.15–4.28 (1H, t, -CH_2-NH-), 3.80–3.87 (2H, d, -CH_2-NH), 3.55 (3H, s, -OCH_3), 3.12 (3H, s, CH_3).^{13}C-NMR [100 MHz, δ, ppm, DMSO-d_6]: 174, 167, 154, 145, 138, 136, 130, 128, 125, 123, 120, 118, 115, 113, 111, 109, 65, 57, 39. ESI-MS: m/z (M^+) 376.

5-[(1H-indol-3-yl)methylene]-3-[(4-hydroxyphenyl)aminomethyl]-1-methylimidazolidine-2,4-dione (5g)

Compound (5g) was obtained as yellow powder analyzed for the yield 70.82%, mp 174–176°C, R_f value is 0.57 from TLC of n-hexane and ethylacetate (9:1). IR spectrum (KBr ν cm^{-1}) showed the characteristic intense bands at 3570 (-OH), 3366 (-NH-), 3254 (-NH-), 1759 (C=O), 1740 (C=O), 1328 (C-N), 2958 (C-H), 3077 (=C-H). ^{1}H-NMR [400 MHz, δ, ppm, DMSO-d_6]: 12.00 (1H, s, indole-NH-), 10.75 (1H, s, phenyl-OH), 8.32 (1H, s, =CH- methylene), 6.89–8.12 (9H, d and t, phenyl-H and indole-H), 4.30–4.42 (1H, t, -CH_2-NH-), 3.95–4.02 (2H, d, -CH_2-NH-), 3.52 (3H, s, CH_3). ^{13}C-NMR [100 MHz, δ, ppm, DMSO-d_6]: 175, 164, 148, 145, 142, 136, 131, 128, 125, 122, 120, 118, 116, 114, 111, 108, 63, 42. ESI-MS: m/z (M^+) 362.

Determination of LD_{50}

Acute oral toxicity studies of the synthesized compounds were conducted in Wistar albino rats (either sex, 6–8 weeks old, weighing 100–120 g) in accordance with the Organization for Economic Co-operation and Development Guideline No. 423 (Acute Toxic Class Method) and under the recommendations of CPCSEA for the care and use of laboratory animals. The animals were acclimatized for seven days under standard laboratory conditions (temperature 25±2°C, relative humidity 45–55%, 12 h light/dark cycle) and housed in clean polypropylene cages with free access to standard pellet diet and water ad libitum. The test compounds were suspended in an appropriate vehicle (0.5% CMC in distilled water) and administered orally by gavage at dose levels of 100, 200, 500, and 1,000 mg/kg body weight to four groups of rats, each comprising six animals.

Based on preliminary toxicity data, the median lethal dose (LD_{50}) of the test compound was estimated to lie between 500 and 1000 mg/kg body weight. Accordingly, the therapeutic dose levels for the pharmacological evaluation were selected on the basis of a standard safety margin. The lowest dose of 100 mg/kg was chosen as approximately $1/10^{th}$ of the estimated LD_{50} value (500 mg/kg), which represents a commonly accepted safety fraction in pharmacological and toxicological studies to ensure non-lethal and subtoxic exposure. The animals were observed individually after dosing for the first 30 min, periodically during the first 24 h, and daily thereafter for a total of 14 days. Observations included mortality, behavioral changes, autonomic and neurological signs, body-weight variations, and gross pathological alterations at necropsy [15,16].

***In vivo* anticonvulsant activity**

To screen for anticonvulsant action in medicines, the most commonly used validated rodent model is PTZ-induced convulsions and maximal

electroshock seizure (MES) tests. By attaching itself to the post-synaptic $GABA_A$ receptor's picrotoxin-binding region, PTZ counteracts GABA's inhibitory effect. Frequent convulsions and depolarization result from this action.

In the investigation, *Wistar albino* rats (150–200 g) of either sex were employed. Sainadh Agencies, Laboratory Animal Suppliers, Hyderabad, is where the animals were acquired. Each group of six animals was created by randomly dividing the animals. Groups of six animals were kept in polypropylene cages with a 12:12 light/dark cycle, at a temperature of 25±1°C and 45–55% relative humidity. Commercial food pellets and unlimited water were given to the animals unless otherwise noted. At least a week before studies, the animals were acclimated to the laboratory environment. The AM Reddy Memorial College of Pharmacy's Institutional Animal Ethical Committee accepted the *in vivo* study's protocols with registration number 1219/PO/Re/S/08/CPCSEA and protocol approval number IAEC/AMRCP/DA/2024/02, both of which were issued on December 28, 2024. Before being given to the animals, all conventional medications and test compounds were dissolved in a 30% w/v aqueous solution of polyethylene glycol (PEG) 400. The dosage of phenytoin was 20 mg/kg, intraperitoneally. An equimolar dose of the synthesized compounds was given in relation to 20 mg/kg of phenytoin. A 30% w/v aqueous solution of PEG 400 was given to the control group [17].

Subcutaneous PTZ (s.c.-PTZ) induced convulsions in Wistar albino rats

The standard group received phenytoin (20 mg/kg), whereas the test group received synthetic hydantoin derivatives (5a–5g) intraperitoneally 1 h before the PTZ challenge. Rats were given PTZ (100 mg/kg, s.c.) after 1 h. The percentage of animals protected, the number of rats that had seizures, and the number of animals protected were all noted [18,19].

Maximal electroshock (MES) test

The most popular test for assessing the anticonvulsant potential of test medications is the MES test, which is used in conjunction with the *s.c.*-PTZ test. This test used a convulsiometer to administer a supramaximal electroshock (50 mA at 60 Hz) through a pair of ocular electrodes for 0.2 s. The positive endpoint was determined to be the extensor reaction of the hind limb. Only rats exhibiting a positive hind limb tonic extensor response were employed after a minimum of 48 h of pre-screening. One hour before the MES challenge, phenytoin (20 mg/kg) and synthetic hydantoin analogs (5a–5g) were injected intraperitoneally [20,21].

Molecular docking studies

Molecular docking experiments were performed on voltage-gated sodium channel target proteins in order to find potential anticonvulsant medicines. A target protein is chosen for docking based on a number of criteria, including having a resolution of 2.0–3.0A°, having a co-crystallized ligand, having its structure established by X-ray diffraction, and not having any protein breaks in its 3D structure [22-24]. Download the PDB files from the RCBS Protein Data Bank (https://www.rcsb.org/) for the 3D crystal structure of voltage-gated sodium channel PDB ID: 3RVY [25,26]. Removing water molecules, adding polar hydrogens, and assigning Gasteiger charges. The docking grid was centered on the active site of the protein with coordinates x=25, y=35, z=40 Å, and the grid box x,y,z dimensions were 28×28×28 Å to ensure full coverage of the binding pocket. The grid spacing was maintained at the Vina default of 0.375 Å. All other parameters were kept at their default settings, and an exhaustiveness value of 8 was used for adequate conformational sampling. Docking results were ranked based on predicted binding affinities (ΔG, kcal/mol), and the top-ranked conformations were analyzed for hydrogen bonds, hydrophobic contacts, and π–π stacking interactions using Discovery Studio Visualizer. Ligands were energy-minimized prior to docking using BIOVIA Discovery Studio Visualizer 2021 to prepare them for docking. The protein structures were stripped down to their lowest energy state by adding polar hydrogens, Kollman charges, and Gasteiger charges in order to make additional analysis easier. Using ChemDraw Ultra 12.0, the intended and generated ligand structures were generated. Chem 3D-Pro 12.0 was then used to reduce and store the structures in SDF file format. SDF file formats for phenytoin standard ligand structure (Pubchem Id: 1775), obtained from the PubChem database. Moreover, Open Babel is used to convert all SDF files to PDB format. Grid-based docking studies with default parameters, protein conversions from PDB to PDBQT file formats, and docking by connecting the protein and ligand using AutoDock Vina were among the activities finished. All docking simulations were performed using the default Lamarckian genetic algorithm parameters, with the exhaustiveness for optimal conformational sampling. The output docking poses were ranked based on predicted binding affinity (ΔG, kcal/mol), and the most favorable pose (lowest binding energy) for each ligand was selected for further analysis. Post-docking visualization and interaction analysis were performed using BIOVIA Discovery Studio Visualizer. The binding interactions, including hydrogen bonds, π–π stacking, amino acid interactions, and hydrophobic interactions, were identified and measured (bond distances in Å). Two-dimensional (2D) interaction diagrams were generated to illustrate the key ligand–receptor contacts. It was feasible to view the docking locations of ligands that connected to the protein active site regions most effectively using the command prompt. With BIOVIA Discovery Studio, the ligand's two-dimensional bindings to the target proteins were observed [27-29].

RESULTS AND DISCUSSION

Chemistry

According to the protocols described in the literature, 1-methyl-imidazolidine-2,4-dione (3) is the product of the Biltz synthesis reaction between glyoxal and N-methyl urea. Condensed with indole-3-aldehyde, 1-methyl-imidazolidine-2,4-dione (3) yielded 5-[(indol-3-yl) methylene]-1-methyl-imidazolidine-2,4-dione (4) under the conditions of the Knoevenagel reaction. After that, compound 4 was combined with formaldehyde and aromatic amines that had been substituted under Mannich reaction conditions to produce the final derivatives 5a–5g that are shown in Fig. 1. Every compound was described both physically and spectrally. According to their percentage yield and reaction time, the physical characterization data are provided in Table 1.

Even after 7 days, it was discovered that the animals in the first and second groups were healthy. Five of the animals in the fourth group passed away within 24 h of the medicine being administered, whereas one of the animals in the third group died 36 h after the treatment was administered. The maximum oral dosage of 1000 mg/kg body weight was shown to be fatal. Therefore, a larger dose of 100 mg/kg body weight of the synthesized compounds, or $1/10^{th}$ of the LD_{50} dose, was chosen for the investigation.

Anticonvulsant activity against s.c.-PTZ induced convulsions

As shown in Table 2, the rats were considerably protected against PTZ-induced convulsions by test compounds 5c and 5d as compared to the control group. In terms of protection percentages, 5c (83.33%) and 5d (66.66%) showed the highest activity of 2,4-dinitrophenyl derivatives. All treated animals were shielded from convulsions by the standard medication phenytoin. The chemicals 5c and 5d were therefore tested further pharmacologically since they showed promise in preventing convulsions in the experimental animals. Comparing the other hydantoin derivatives to the regular phenytoin, a moderate amount of protection was demonstrated.

Anti-convulsant activity against maximal electroshock (MES) test

According to Table 3, the mice in this test were shielded from MES-induced seizures by the synthetic hydantoin derivatives 5a, 5c, and 5d, which included the common medication phenytoin. In terms of protection percentages, 5a (66.66%), 5c (83.33%), and 5d (83.33%) showed the highest activity. Standard phenytoin and developed compounds that are chemically related to it have been shown to be effective in preventing seizures and to produce a protective effect in MES. Tonic hind limb extension mortality rate, incidence, and latency were noted.

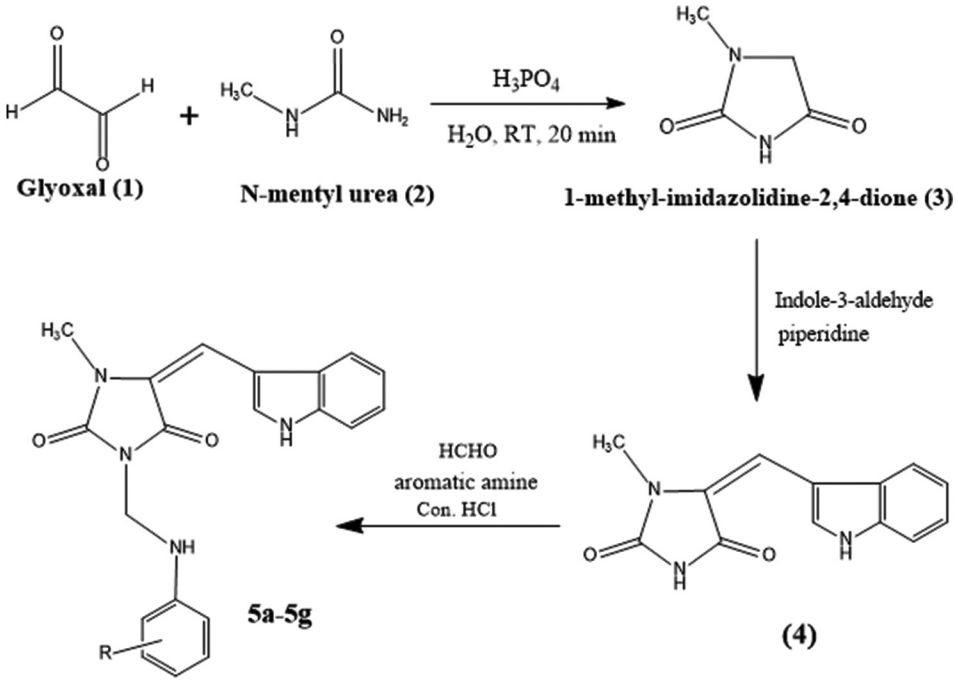

Fig. 1: Scheme of synthesis of hydantoin derivatives (5a–5g)

Table 1: Physical characterization data of developed hydantoin derivatives 5a–5g

Compd.	R	m.p. (°C)	Molecular formula	mol. wt.	Percentage yield	R_f value
5a	4-bromo	184–186	$C_{20}H_{17}BrN_4O_2$	425.28	68.42	0.53
5b	4-chloro	190–192	$C_{20}H_{17}ClN_4O_2$	380.83	70.25	0.57
5c	2,4-dinitro	204–206	$C_{20}H_{16}N_6O_6$	436.38	69.10	0.62
5d	4-nitro	194–196	$C_{20}H_{17}N_5O_4$	391.38	73.41	0.54
5e	4-methoxy	188–190	$C_{21}H_{23}N_4O_3$	376.41	70.67	0.51
5f	4-methyl	200–202	$C_{21}H_{20}N_4O_2$	360.41	68.36	0.56
5g	4-hydroxy	174–176	$C_{21}H_{18}N_4O_3$	362.38	70.82	0.57

Table 2: Anticonvulsant activity of test compounds against PTZ-induced convulsions

S. No.	Group	Latency of tonic convulsions±SEM (min)	Number of animals protected	Percentage protection
1	Control	7.56±1.21	0/6	0.00
2	5a	10.65±0.76*	3/6	50.00
3	5b	8.41±1.15*	2/6	33.33
4	5c	14.52±0.98	5/6	83.33
5	5d	13.84±1.06**	4/6	66.66
6	5e	7.99±0.64	2/6	33.33
7	5f	8.72±1.11	2/6	33.33
8	5g	11.64±0.86	3/6	50.00
9	Phenytoin	15.03±1.25*	6/6	100.00

Values are expressed as the Mean±SEM (n=6); *p<0.05, **p<0.01 when compared to respective control values by ANOVA+Dunnett's *post hoc* test. Control: 30% w/v PEG400 in distilled water; Phenytoin: (20 mg/kg, *i.p*) in 30% w/v PEG400 in distilled water; test compounds (5a–5g) were administered at an equimolar intraperitoneal dose relative to 20 mg/kg phenytoin in 30% w/v PEG400 in distilled water. SEM: Scanning electron microscope, ANOVA: Analysis of variance

Table 3: Anticonvulsant activity of test compounds against MES-induced convulsions

S. No.	Group	Mean duration of tonic hind leg extension±SEM (s)	Number of animals protected	Percentage protection
1	Control	10.32±1.07	0/6	0
2	5a	8.57±0.43**	4/6	66.66
3	5b	13.86±1.04*	2/6	33.33
4	5c	4.56±0.61**	5/6	83.33
5	5d	5.12±0.85*	5/6	83.33
6	5e	11.19±1.12**	3/6	50.00
7	5f	11.67±0.71*	3/6	50.00
8	5g	13.95±0.15*	2/6	33.33
9	Phenytoin	0.00±0.00	6/6	100.00

Values are expressed as the Mean±SEM (n=6); *p<0.05, **p<0.01 when compared to respective control values by ANOVA+Dunnett's *post hoc* test. Control: 30% w/v PEG400 in distilled water; Phenytoin: (20 mg/kg, *i.p*) in 30% w/v PEG400 in distilled water; Test compounds (5a–5g) were administered at an equimolar intraperitoneal dose relative to 20 mg/kg phenytoin in 30% w/v PEG400 in distilled water. SEM: Scanning electron microscope, ANOVA: Analysis of variance

The present study employed a relatively small sample size (n=6 per group), which, although commonly used in preliminary pharmacological investigations, may limit the statistical power and generalizability of the findings. Future studies with larger animal cohorts are warranted to confirm the reproducibility of these results and to strengthen the statistical significance of observed effects.

Docking at voltage-gated sodium ion channels (PDB: 3RVY)

The hydantoin derivatives' hydrogen bonding interactions, both in terms of frequency and strength, provide insight into molecular compatibility, which is probably related to how well the ligands work at voltage-gated sodium ion channels.

Molecular docking of the synthesized compounds and phenytoin with human voltage-gated sodium channel (PDB: 3RVY) revealed a range of predicted binding affinities, with compound 5b showing the strongest interaction (ΔG=−9.5 kcal/mol) and phenytoin exhibiting a binding energy of −8.0 kcal/mol. All ligands formed a combination of hydrogen bonds, π-π stacking interactions, and hydrophobic contacts with key residues in the binding pocket, such as PHE1171, TRP2195, and ILE2199. For example, 5b formed two hydrogen bonds with PHE1171, multiple π-π stacking interactions with TRP2195 and PHE1167, and hydrophobic contacts with ILE2199 and PHE2203. Compounds 5c and 5d also exhibited multiple stabilizing interactions within the active site, consistent with their high predicted binding affinities (−9.1 kcal/mol). Phenytoin, as the reference compound, displayed hydrogen bonding with TRP2195 and π-π stacking with PHE1167, supporting its known anticonvulsant activity. Detailed 2D interaction diagrams for each ligand are presented in Fig. 2, showing hydrogen bonds, π-π stacking, and hydrophobic contacts along with interatomic distances in Å. A closer look at the specific information in Table 4 shows that hydrogen-bond interactions are nevertheless important for some hydantoin derivatives' binding affinity to voltage-gated sodium ion

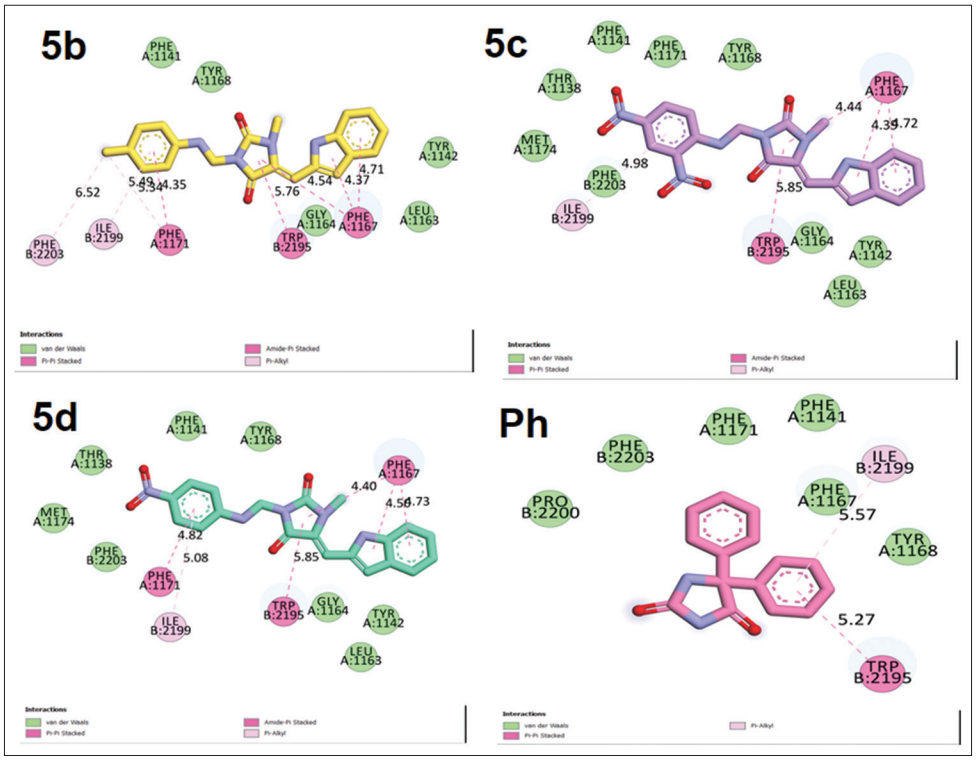

Fig. 2: 2D view interaction of 5b, 5c, 5d, and Ph (phenytoin) at 3RVY protein target

Table 4: Binding energies and interaction of designed ligands with voltage-gated sodium ion channels (PDB: 3RVY)

Ligand	Binding energy (ΔG, kcal/mol)	Interaction type	Amino acid residue	Atom involved	Distance (Å)
5a	−7.9	H-bond	TRP B: 2195	N-H…O	3.21
		π-π stacking	PHE A: 1153	Aromatic ring	4.42
		Hydrophobic	PHE A: 1151, ILE B: 2186	Side chain	4.55–5.36
5b	−9.5	H-bond	PHE A: 1171	O…H	3.08, 3.25
		π-π stacking	TRP B: 2195, PHE A: 1167	Aromatic ring	4.50–4.78
		Hydrophobic	ILE B: 2199, PHE B: 2203	Side chain	4.35–5.49
5c	−9.1	H-bond	TRP A: 2195	N-H…O	3.15
		π-π stacking	PHE A: 1167	Aromatic ring	4.44–4.72
		Hydrophobic	ILE A: 2199	Side chain	4.39–4.98
5d	−9.1	H-bond	PHE A: 1171	O-H…O	3.12
		π-π stacking	TRP B: 2195	Aromatic ring	4.50–5.10
		Hydrophobic	ILE B: 2199, PHE A: 1167	Side chain	4.40–4.82
5e	−6.9	H-bond	MET A: 1174	S-H…O	3.25
		π-π stacking	PHE A: 1171	Aromatic ring	4.38–4.57
		Hydrophobic	PHE B: 2203, ILE B: 2199	Side chain	4.38–5.34
5f	−7.0	H-bond	TYR A: 1168	O-H…O	3.2
		π-π stacking	TRP B: 2195	Aromatic ring	4.22–5.15
		Hydrophobic	ILE B: 2199, PHE A: 1167	Side chain	4.24–5.35
5g	−7.3	H-bond	TRP B: 2195	N-H…O	3.18
		π-π stacking	PHE A: 1167, PHE A: 1171	Aromatic ring	4.32–4.71
		Hydrophobic	ILE A: 2199	Side chain	4.36–5.59
Phenytoin	−8.0	H-bond	TRP B: 2195	N-H…O	3.12
		π-π stacking	PHE A: 1167	Aromatic ring	4.5
		Hydrophobic	ILE B: 2199	Side chain	4.57–5.57

channels. These interactions help the ligand's specificity and docking stability, which may improve their pharmacological effects even though they are weaker than hydrogen bonds and van der Waals forces.

CONCLUSION

This study used the Biltz, Knoevenagel, and Mannich reactions to create a variety of hydantoin derivatives with indole and substituted phenyl appendages. Physical and spectroscopic characterizations of the synthesized substances were performed. *In vivo* anticonvulsant activity evaluated using methods such as PTZ and MES tests indicates that 5c and 5d exhibited promising anticonvulsant activity, found to be the most active compounds. Molecular docking studies at the voltage-gated sodium channel target, compounds 5b, 5c, and 5d, demonstrated noteworthy binding affinities.

The structure–activity relationship (SAR) analysis of the synthesized compounds (5a–5g) indicates that the presence and position of electron-withdrawing substituents, particularly the nitro ($-NO_2$) group, play a significant role in enhancing anticonvulsant activity. Compounds bearing such substituents (e.g., 5b, 5c, and 5d) demonstrated stronger binding affinities in molecular docking ($\Delta G \approx -9.1$ to -9.5 kcal/mol) and higher *in vivo* protection percentages compared to their unsubstituted or electron-donating analogs. This enhancement can be mechanistically explained by several interrelated factors. First, electron-withdrawing groups reduce the electron density on the aromatic ring, facilitating π–π stacking and hydrophobic interactions with aromatic residues such as PHE1171 and TRP2195 within the target protein's binding site. This improved electronic complementarity strengthens ligand–receptor interactions, contributing to lower binding energies. Second, the introduction of polar groups such as $-NO_2$ enhances dipole–dipole and hydrogen bonding capabilities, allowing additional interactions with key amino acid residues. Third, the increased lipophilicity and membrane permeability associated with moderately electron-withdrawing substituents may favor efficient penetration across the blood–brain barrier, which is critical for anticonvulsant efficacy. In contrast, analogs bearing weakly electron-donating or bulky substituents displayed reduced activity, likely due to unfavourable steric hindrance and diminished polar interaction potential. Collectively, these findings suggest that the electron-withdrawing strength and steric orientation of substituents critically influence both binding affinity at the sodium channel active site and pharmacokinetic behavior, offering a rational basis for future structural optimization of this scaffold toward potent anticonvulsant agents.

An important observation emerging from this study is the notable discrepancy between the strong *in silico* binding affinity of compound 5b ($\Delta G = -9.5$ kcal/mol) and its relatively modest *in vivo* anticonvulsant protection (33.33%) in the PTZ-induced seizure model. While molecular docking results suggest a high theoretical affinity toward the sodium channel active site (PDB: 3RVY), this does not necessarily guarantee equivalent pharmacological efficacy *in vivo*. Several factors may contribute to this divergence. First, pharmacokinetic limitations such as poor absorption, suboptimal blood–brain barrier permeability, rapid metabolism, or inadequate bioavailability may prevent the compound from achieving sufficient central nervous system concentrations to elicit a significant anticonvulsant effect. Second, the mechanistic mismatch between models may also explain the reduced PTZ protection. The docking studies targeted the voltage-gated sodium channel, which is primarily associated with the maximal electroshock (MES) model of seizure suppression. In contrast, the PTZ model predominantly reflects modulation of the GABAergic neurotransmission pathway. Therefore, compound 5b may act more selectively on sodium channel-mediated neuronal stabilization, leading to limited efficacy in the PTZ model, which emphasizes GABA receptor modulation. In addition, it is possible that metabolic instability or rapid clearance *in vivo* compromises its active concentration, despite favorable *in silico* interactions. This finding underscores the importance of integrating pharmacokinetic and mechanistic studies alongside docking and behavioral assays. Future studies incorporating ADME profiling, plasma stability assays, and multimodel anticonvulsant screening will be essential to clarify the functional relevance of the high docking affinity observed for compound 5b. Both *in-vivo* anticonvulsant and *in silico* docking investigations state that, among the tested analogs, compounds 5c and 5d emerge as the most promising scaffolds for further optimization and advanced pharmacological evaluation.

ACKNOWLEDGMENTS

The authors are thankful to Acharya Nagarjuna University, Guntur; Krishna University College of Pharmaceutical Sciences and Research, Machilipatnam, and AM Reddy Memorial College of Pharmacy, Narasaraopet, Andhra Pradesh, for providing the necessary facilities to carry out the research work.

AUTHOR CONTRIBUTIONS

Dandamudi Alekhya: Conceptualization of the study, design and execution of *in vivo* anticonvulsant experiments, data collection, analysis, interpretation of results, and preparation of the initial draft of the manuscript. Konda Ravi Kumar: Supervision of the research work, guidance in molecular docking studies, critical review and editing of the manuscript, interpretation of SAR and docking *in vivo* correlations.

CONFLICTS OF INTEREST

The authors have no conflict of interest to declare.

FUNDING

This research did not receive any funding.

REFERENCES

1. Wadghane S, Bhor R, Shinde G, Kolhe M, Rathod P. A review on the some biological activities of the hydantoin derivatives. J Drug Deliv Ther. 2023;13(1):171-8. doi: 10.22270/jddt.v13i1.5904
2. Gawas PP, Ramakrishna B, Veeraiah N, Nutalapati V. Multifunctional hydantoins: Recent advances in optoelectronics and medicinal drugs from Academia to the chemical industry. J Mater Chem C. 2021;9(46):16341-77. doi: 10.1039/d1tc04090a
3. Padwa A, Bur SK. The domino way to heterocycles. Tetrahedron. 2007;63(25):5341-78. doi: 10.1016/j.tet.2007.03.158, PMID 17940591
4. Peerzada MN, Hamel E, Bai R, Supuran CT, Azam A. Deciphering the key heterocyclic scaffolds in targeting microtubules, kinases and carbonic anhydrases for cancer drug development. Pharmacol Ther. 2021;225:107860. doi: 10.1016/j.pharmthera.2021.107860, PMID 33895188
5. Brunton L, Parker K, Blumenthal D, Buxton I. Goodman and Gilman's Manual of Pharmacology and Therapeutics. New York: McGraw-Hill; 2008. doi: 10.1036/0071443436
6. Lingappa M, Guruswamy V, Bantal V. Synthesis and characterization of 4-amino-4H-1,2,4-triazole derivatives: Anticonvulsant activity. Curr Chem Lett. 2021;10(1):33-42. doi: 10.5267/j.ccl.2020.7.002
7. Hassanin MA, Mustafa M, Abourehab MA, Hassan HA, Aly OM, Beshr EA. Design and synthesis of new hydantoin acetanilide derivatives as anti-NSCLC targeting EGFRL858R/T790M mutations. Pharmaceuticals (Basel). 2022;15(7):857. doi: 10.3390/ph15070857
8. Chin EZ, Tan SP, Liew SY, Kurz T. Synthesis and characterization of amino acid-derived hydantoins. Malays J Chem. 2021;23(2):19-25.
9. Konnert L, Lamaty F, Martinez J, Colacino E. Recent advances in the synthesis of hydantoins: The state of the art of a valuable scaffold. Chem Rev. 2017;117(23):13757-809. doi: 10.1021/acs.chemrev.7b00067, PMID 28644621
10. Baccolini G, Boga C, Delpivo C, Micheletti G. Facile synthesis of hydantoins and thiohydantoins in aqueous solution. Tetrahedron Lett. 2011;52(14):1713-7. doi: 10.1016/j.tetlet.2011.02.002
11. Brackman G, Al Quntar AA, Enk CD, Karalic I, Nelis HJ, Van Calenbergh S, *et al*. Synthesis and evaluation of thiazolidinedione and dioxazaborocane analogues as inhibitors of AI-2 quorum sensing in *Vibrio harveyi*. Bioorg Med Chem. 2013;21(3):660-7. doi: 10.1016/j.bmc.2012.11.055, PMID 23286963
12. Srikanth Kumar K, Lakshmana Rao A, Basaveswara Rao MV. Design, synthesis, biological evaluation and molecular docking studies of

novel 3-substituted-5-[(indol-3-yl)methylene]-thiazolidine-2,4-dione derivatives. Heliyon. 2018;4(9):e00807. doi: 10.1016/j.heliyon.2018.e00807, PMID 30258996

13. Alexander ER, Underhill EJ. Studies on the mechanism of the mannich reaction. I. Ethylmalonic acid, a methynyl compound. J Am Chem Soc. 1949;71(12):4014-9. doi: 10.1021/ja01180a041
14. Jiwane SK, Singh VK, Namdeo KP, Prajapati SK. Synthesis of some novel 2,4-thiazolidinedione derivatives and their biological screening as antidiabetic agents. Asian J Chem. 2009;21:5068-72.
15. Enoch OC, Ezeonu CF. Comparative study of LD50 determination of bisphenol A in Albino Wistar rats using different method. Asian Sci Bul. 2024;2(1):92-8. doi: 10.3923/asb.2024.92.98
16. Raj A, Nair NS, Nisha AR, Sujith S, Divya C, Shankar R. Determination of the median lethal dose of indoxacarb pesticide in Wistar rat. J Vet Anim Sci. 2023;54(2):510-5. doi: 10.51966/jvas.2023.54.2.510-515
17. Singh RB, Das N, Singh GK, Singh SK, Zaman K. Synthesis and pharmacological evaluation of 3-[5-(aryl-[1,3,4] oxadiazole-2-yl]-piperidine derivatives as anticonvulsant and antidepressant agents. Arab J Chem. 2020 May 1;13(5):5299-311. doi: 10.1016/j.arabjc.2020.03.009
18. Fakhrioliaei A, Abedinifar F, Salehi Darjani P, Mohammadi-Khanaposhtani M, Larijani B, Ahangar N, *et al*. Hybridization of the effective pharmacophores for treatment of epilepsy: Design, synthesis, *in vivo* anticonvulsant activity, and *in silico* studies of phenoxyphenyl-1,3,4-oxadiazole-thio-N-phenylacetamid hybrids. BMC Chem. 2023 Jul 17;17(1):80. doi: 10.1186/s13065-023-01000-6, PMID 37461080
19. Dehestani L, Ahangar N, Hashemi SM, Irannejad H, Honarchian Masihi PH, Shakiba A, *et al*. Design, synthesis, *in vivo* and *in silico* evaluation of phenacyl triazole hydrazones as new anticonvulsant agents. Bioorg Chem. 2018 Aug 1;78:119-29. doi: 10.1016/j.bioorg.2018.03.001, PMID 29550532
20. Bettio L, Bankar G, Dube CM, Nelkenbrecher K, Filipovic M, Singh S, *et al*. The pharmacokinetic and pharmacodynamic relationship of clinically used antiseizure medications in the maximal electroshock seizure model in rodents. Int J Mol Sci. 2025;26(15):7029. doi: 10.3390/ijms26157029, PMID 40806162
21. Botros S, Khalil NA, Naguib BH, El-Dash Y. Synthesis and anticonvulsant activity of new phenytoin derivatives. Eur J Med Chem. 2013 Feb 1;60:57-63. doi: 10.1016/j.ejmech.2012.11.025, PMID 23287051
22. Khirallah SM, Ramadan HM, Shawky A, Qahl SH, Baty RS, Alqadri N, *et al*. Development of novel 1,3-Disubstituted-2-Thiohydantoin analogues with potent anti-inflammatory activity; *in vitro* and *in silico* assessments. Molecules. 2022;27(19):6271. doi: 10.3390/molecules27196271, PMID 36234810
23. Baba H, Bunu SJ. Spectroscopic and molecular docking analysis of phytoconstituent isolated from *Solenostemon monostachyus* as potential cyclooxygenase enzymes inhibitor. Int J Chem Res. 2025 Jan 9;1:1-6. doi: 10.22159/ijcr.2025v9i1.241
24. Nagre R, Buwa V. Molecular docking studies of monomeric wildtype and mutant. Int J Chem Res. 2022 Oct 6;H81a(H49r):5-13. doi: 10.22159/ijcr.2022v6i4.207
25. Das D, Kumar A, Guruprasad R, Mahapatra DK. Molecular docking and density function theory (DFT) studies of some 4-(2-chloroacetamido) benzoic acid derivatives as local anesthetics. J Mol Model. 2017;2021:1-5.
26. Hompoonsup S. Identification and Transcriptional Characterization of Novel Inhibitors of NAv1. 7 and TRKB. London: King's College London; 2018.
27. Karumanchi SK, Atmakuri LR, Mandava VB, Rajala S. Synthesis and hypoglycemic and anti-inflammatory activity screening of novel substituted 5-[morpholino(phenyl)methyl]-thiazolidine-2,4-diones and their molecular docking studies. Turk J Pharm Sci. 2019 Dec;16(4):380-91. doi: 10.4274/tjps.galenos.2018.82612, PMID 32454740
28. Kurian TK. *In silico* screening by molecular docking of heterocyclic compounds with furan or indole nucleus from database for anticancer activity and validation of the method by redocking. Int J Pharm Pharm Sci. 2024 Apr;16(4):42-5. doi: 10.22159/ijpps.2024v16i4.50478
29. Aiswariya SB, Satya MS. Molecular docking and ADMET studies of benzotriazole derivatives tethered with isoniazid for antifungal activity. Int J Curr Pharm Res. 2022 Jul;14(4):78-80. doi: 10.22159/ijcpr.2022v14i4.2004%20